Chaos
An Interdisciplinary Journal of Nonlinear Science

RESEARCH ARTICLE | JULY 17 2023

Criticality in transient behavior of coupled oscillator system toward chimera and synchronization

Special Collection: Chimera states: from theory and experiments to technology and living systems

Nan Yao ; Qian-Yun Zhang ; De-Yi Ren ; You-Jun Li; Chun-Wang Su ; Zhong-Ke Gao ; Jürgen Kurths

Chaos 33, 073131 (2023)
https://doi.org/10.1063/5.0152858

AIP Publishing

Chaos ARTICLE pubs.aip.org/aip/cha

Criticality in transient behavior of coupled oscillator system toward chimera and synchronization

Cite as: Chaos 33, 073131 (2023); doi: 10.1063/5.0152858
Submitted: 2 April 2023 · Accepted: 29 June 2023 ·
Published Online: 17 July 2023 · Corrected: 20 July 2023

View Online Export Citation CrossMark

Nan Yao,[1] Qian-Yun Zhang,[2] De-Yi Ren,[2] You-Jun Li,[2] Chun-Wang Su,[2,a)] Zhong-Ke Gao,[3] and Jürgen Kurths[4,5]

AFFILIATIONS

[1] Department of Applied Physics, Xi'an University of Technology, Xi'an 710054, China
[2] School of Life Science and Technology, Xi'an Jiao Tong University, Xi'an 710049, China
[3] School of Electrical and Information Engineering, Tianjin University, Tianjin 300072, People's Republic of China
[4] Potsdam Institute for Climate Impact Research, Telegraphenberg A31, 14473 Potsdam, Germany
[5] Department of Physics, Humboldt University Berlin, 12489 Berlin, Germany

Note: This paper is part of the Focus Issue on Chimera states: from theory and experiments to technology and living systems.

[a)] **Author to whom correspondence should be addressed:** Suchunwang@xjtu.edu.cn

ABSTRACT

Chimera states in spatiotemporal dynamical systems have been investigated in physical, chemical, and biological systems, while how the system is steering toward different final destinies upon spatially localized perturbation is still unknown. Through a systematic numerical analysis of the evolution of the spatiotemporal patterns of multi-chimera states, we uncover a critical behavior of the system in transient time toward either chimera or synchronization as the final stable state. We measure the critical values and the transient time of chimeras with different numbers of clusters. Then, based on an adequate verification, we fit and analyze the distribution of the transient time, which obeys power-law variation process with the increase in perturbation strengths. Moreover, the comparison between different clusters exhibits an interesting phenomenon, thus we find that the critical value of odd and even clusters will alternatively converge into a certain value from two sides, respectively, implying that this critical behavior can be modeled and enabling the articulation of a phenomenological model.

Considering the generality of chimera, an issue of both theoretical and experimental interest is the generation of stable chimera states through a transient time responding to perturbation. Here, we uncover general critical behavior and transition from chimera to synchronization that occurs in the transient processes of coupled oscillators under perturbation. It was also found that the critical value of odd- and even-cluster systems alternatively converge into a certain value, implying that this critical behavior can be modeled and enabling the articulation of a phenomenological model. Our work provides a clear physical and dynamical picture on how the criticality in the transient behavior of either chimera or synchronization takes place.

I. INTRODUCTION

An chimera state is a spatiotemporal pattern, in which a system of identical oscillators is split into coexisting regions of coherent and incoherent oscillation. It was found by Kuramoto in 2002,[1] and named by Abrams and Strogatz.[2,3] In real-word systems, this phenomenon might play a role in the hemispherical sleep of Marine mammals or birds,[4,5] in neural spikes,[6,7] in power grids,[8] in social systems,[9] or possibly in ventricular fibrillations[10] and epileptic seizures.[11] Therefore, it is of high significance to study chimera states. At first, a great deal of research was focused on chimera states in regular networks of phase-coupled oscillators with one-dimensional chain or ring topology,[1,2,12] and networks with limit populations.[13,14] Subsequent research found that this peculiar phenomenon can be found on two-dimensional planes,[3,15] three-dimensional lattices,[16] torus,[17,18] and systems with a spherical topology.[19] With the in-depth research, many issues like effects of transient behaviors,[20–22] time delay,[23–25] phase lags,[26] criteria for state optimization,[27] coupling functions,[28–32] and the impacts of specific driven forces,[33] random perturbation and complex topology of coupling[34–38] have been solved, e.g., the emergence of chimera states in modular networks,[39] the association between synchronization dynamics and eigenvectors of coupling matrix,[40] and the optimal control strategies based on susceptible direction identification.[41] Thus, the survival conditions of chimera states have been continuously expanded. Then, it was discovered that the emergence of chimera states is not limited to the Kuramoto phase oscillators, but can also be observed in the Landau–Stuart and the Ginzburg–Landau systems,[25,42–49] chaotic maps,[50] quantum oscillator systems,[51,52] time-continuous Rössler,[53,54] Lorenz,[55] and neural networks such as Hodgkin–Huxley, FitzHugh–Nagumo, and Integrate-and-Fire oscillators.[56–59] Besides widely numerical and theoretical studies, experimental evidence of chimera states has been presented in optical,[60,61] chemical,[62–64] mechanical,[65] electronic,[66,67] and electrochemical[68] setups.

An interesting finding is that chimera states can be considered long living transients toward the in-phase synchronization. It was experimentally confirmed that the lifetime of a chimera grows exponentially with the system size.[21] Since the size of the systems in nature is limited, various spatial characteristics of chimera states can be observed, such as Traveling chimera,[69,70] Breathing chimera,[71,72] Spiral wave chimera,[73,74] and Imperfect traveling chimera.[75] Next to the classical chimera state, which exhibits one coherent phase-locked and one incoherent region, there exists a new class of dynamics that possesses multiple domains of incoherence. In this regard, two clusters can be observed in coupled oscillator systems, using symmetric Gaussian initial phase.[26] Stable 4-cluster chimera states are obtained by adding an external force to the coupling system or introducing time-delay.[24,76] Different phase lags α in the general non-locally coupled system,[30] for the special form of the nonlocally coupling function $G(x - x')$,[29,69] can also induced a variety of phase clustering. Moreover, these multi-chimera states can arise in a transition from classical chimera states, depending on the coupling strength and range.[28]

Chimera states in spatiotemporal dynamical systems have been investigated in physical, chemical, and biological systems, and have been shown to be robust against random perturbations. The robustness of chimera states have been discussed by studying the effects of random removal of links between oscillators.[35] Iryna Omelchenko's research demonstrated that chimera states exhibit strong robustness in the presence of perturbations in coupling topologies. The properties of chimera states as the level of inhomogeneity increases were also analyzed.[77] Malchow demonstrated that chimera patterns persist for inhomogeneous parameters.[78] Recently, basin stability on chimera states and how to quantify their stability after even large perturbations have been investigated.[79] Furthermore, it has been discovered that chimera states exhibit a self-adaptive behavior in the presence of spatially localized perturbations. The coherent centers of the chimera spontaneously drift toward an optimal location as far away from the perturbation as possible, aiming to minimize the impact of the perturbation.[80]

Actually, most of the previous researches predominantly focused on examining the properties, formation conditions, and patterns of chimera states. In this paper, we focus on the process of how does the system respond to perturbations before entering the new stable state. We will discuss for different final regimes of the system, how long does it take to enter a new stable state (chimera or synchronization).

The rest of the paper is organized as follows: In Sec. II, we introduce the model equations, the order parameter, and the perturbation method that we use. In Sec. III, after a brief review of results and new aspects on the chimera states, we do experiments on multi-cluster chimeras and analyze the critical behavior of a coupled oscillator system in transient time toward chimera and synchronization. In particular, we explore how does the system respond to perturbations before entering the new stable state on the basis of spatiotemporal patterns, transient time, and analyze the critical perturbation strength on the basis of the order parameter, plots of the transient time, and bifurcation diagrams. Then, we fit the changing trend to get further descriptions. In Sec. IV, we predict the unknown critical values of larger clusters and describe an interesting phenomenon based on the comparison plots and a convergence phenomenon. Finally, we summarize our study in Sec. V.

II. THE MODEL

In this article, we consider a one-dimensional network of nonlocally coupled, identical phase oscillators with periodic boundary condition (a ring configuration). The system is mathematically described as

$$\frac{d\phi\left(x_i\right)}{dt} = \omega - \frac{2\pi}{N}\sum_{j=1}^{N} G\left(x_i - x_j\right)\sin\left[\phi\left(x_i\right) - \phi\left(x_j\right) + \alpha\right], \quad (1)$$

where $\phi(x_i)$ is the phase of the ith oscillator at the spatial location x_i and N denotes the size of the oscillator system. The angular velocity ω and phase lag α of the oscillators are constants in space. Without loss of generality, we set $\omega = 0$ and $\alpha = \pi/2 - 0.18$, which are slightly less than $\pi/2$. To induce multi-chimera states, we consider the widely used kernel function, with an extra parameter "n" for n-cluster chimera: $G(x_i - x_j) = [1 + A\cos n\left(x_i - x_j\right)]/2\pi$, which is a non-negative even function that characterizes the nonlocal coupling among the oscillators. In this function, A is set to $A = 0.995$, which was chosen based on early references, to ensure the occurrence of chimera states and prevent the kernel function from becoming 0 for any $(x_i - x_j)$ value. As the value of A decreases, the existence domain of the 2-cluster chimera becomes smaller, and when $A < 0.8$, this domain no longer exists.[2,12,26] The initial condition is generated using the function $f(x) = 6r \cdot \exp(-0.76x^2)$, where r is a random variable uniformly distributed in $[-1/2, 1/2]$.

The complex order parameter $Z(x_i)$ defined for oscillator i can be used to characterize the dynamics of the system,[1]

$$Z(x_i) \equiv R\left(x_i\right) e^{i\Theta(x_i)} = \frac{2\pi}{N}\sum_{j=1}^{N} G\left(x_i - x_j\right) e^{i\theta\left(x_j\right)}. \quad (2)$$

The global order parameter R, which varies with time and space, is a macroscopic quantity that can be interpreted as the collective rhythm produced by the whole population. The value of R represents the level of synchronization of the system, with $0 \leqslant R(t) \leqslant 1$. A higher value of R indicates that the oscillators in the system are more synchronized, and $R = 1$ corresponds to a global synchronization state (phase locking). While the lower values indicate more disorder, and when $R = 0$, the oscillators run incoherently. Looking closer at the phase dynamics, the observed behavior of $0 < R < 1$ is the consequence of complex spatiotemporal patterns, in which in-phase synchronous domains coexist with asynchronous ones. In this case, the coherent centers are identified by calculating the local order parameters $R(x_i)$. The oscillator with local maximum value of $R(x_i)$ is considered the coherent centers, and in a n-cluster chimera, we would find n coherent centers.

Since the oscillator network has periodic boundary conditions, choosing different coherent centers will yield similar experimental results. Therefore, in Secs. III A–III C, we randomly select one of the coherent centers (m_c) as a representative for subsequent perturbation experiments and analysis. To assess how perturbations affect the chimera states, we apply a phase perturbation to four target oscillators (m_1, m_2, m_3, m_4) beside that coherent center m_c that $m_1 = m_c - 1, m_2 = m_c, m_3 = m_c + 1, m_4 = m_c + 2$, where m represents the index of the oscillators, ranging from 1 to N. The nature of the perturbation is to force upon the oscillator a constant phase difference $\Delta\phi$ with respect to the local mean phase $\bar{\phi}_{\text{local}}$ of its neighbors, with an equal number of neighbors on the left and right sides. Namely, $\phi\,(x_m, t) = \bar{\phi}_{\text{local}}(x_m) + \Delta\phi$ for those perturbation points. The evolution and relaxation process of chimera states under phase perturbations can be analyzed by observing spatiotemporal patterns, phase plots, and snapshots, and by measuring the phase velocities, the relaxation, and the transient time, etc.

III. RESULTS

In this paper, numerical simulations are conducted in a one-dimensional network of $N = 240$ non-locally coupled identical phase oscillators with periodic boundary condition. Through setting $n = 1, 2, 3, 4, 5$ in the coupling function $G(x_i - x_j)$, one can generate chimera states consisting of n clusters. We apply phase perturbations to four oscillators located at the center of the system, where the initial condition is set to be a coherent center of the chimera. Figure 1 shows the spatiotemporal patterns of 1, 2, 3, 4, 5-cluster chimera, in response to perturbations at four target oscillators with increasing strength $\Delta\phi$.

A. Two different destinies of the system under perturbation

According to the spatiotemporal pattern of oscillators, it can be found that after a period of transient time, the system evolves from the initial condition to a certain stable state. The final stable state would either be chimera or synchronization, depending on the strength of the perturbation $\Delta\phi$ (see Fig. 1).

For the case with small perturbation strength $\Delta\phi$ (as is shown in the left-hand side panels in Fig. 1), the system will enter the chimera state after a self-adaption transient process, in which the global order parameter of the n-cluster chimera and the boundary between incoherent and coherent regions gradually evolved to its stability.

However, for the case with large enough perturbation strength $\Delta\phi$ (as is shown in the right-hand side panels in Fig. 1), the chimera state will collapse and the in-phase synchronized oscillatory state takes over. We conjecture that this phenomenon occurs for the reason that the basin of chimera is typically relatively small, with respect to that of the synchronization. Strong perturbations on oscillators destabilize these multi-cluster chimera states, and thus promote global synchronization.

B. The critical value of the perturbation strength

As mentioned above, stronger perturbations lead to a phase transition from chimera to synchronization. But how to describe the influence of perturbations $\Delta\phi$ is worth to be further studied.

First, the transient time (T) is defined as the duration from the moment of perturbation to the occurrence of a stable chimera or synchronization states. By observing the spatiotemporal pattern and the variation of R, we have found that when the chimera state is reached, R will fluctuate regularly around a certain value as a breathing chimera with a stable rhythm. Therefore, the transient time T of a chimeras is from the initial moment to the moment that R starts to behave as a breathing chimera. However, if the global order parameter R cannot exhibit regular fluctuations and instead gradually converges to $R = 1$, it indicates that the system enters a fully synchronized state instead of a chimera. Hence, from the initial moment to R approaches 1 is the transient time before reaching the fully synchronized state.

We sweep the perturbation strength from 0 to π with a step size of 0.01π and apply the perturbation to the target oscillator in the chimera state. Then, we observe the spatiotemporal patterns of the system's evolution at each perturbation strength. From the spatiotemporal patterns, we can clearly see the state in which the system maintains after a certain period of evolution. As the perturbation strength increases, the time for the system to recover the chimera state gradually lengthens and extends to infinity, until it exceeds a certain perturbation threshold $\Delta\phi_c$. Beyond this threshold, the system cannot recover the chimera state and transitions to a fully synchronized state. This pertubation threshold can be considered the critical value $\Delta\phi_c$ between these two possible final states. When the perturbation strength is less than $\Delta\phi_c$, the system can resist the perturbation through self-adaptations; however, when the perturbation strength is greater than $\Delta\phi_c$, chimera collapses and is replaced by synchronization, instead of making adaptive adjustments.

For each cluster's chimera, we calculated the critical values of perturbation strength under ten different initials, denoted as $(\Delta\phi_{cn_1}, \ldots, \Delta\phi_{cn_{10}}$, where n represents the cluster number, and 1–10 correspond to the ten initial groups). The critical value of that cluster's chimera is the average of these ten initial groups: $\Delta\phi_{cn} = avg(\Delta\phi_{cn_1}, \ldots, \Delta\phi_{cn_{10}})$. Since the results were obtained from multiple experiments with ten sets of initial values, and the transient time curves exhibit consistent trends for different initial values, averaging all the trials provides a more accurate estimation of the critical value for that specific cluster's chimera. In addition,

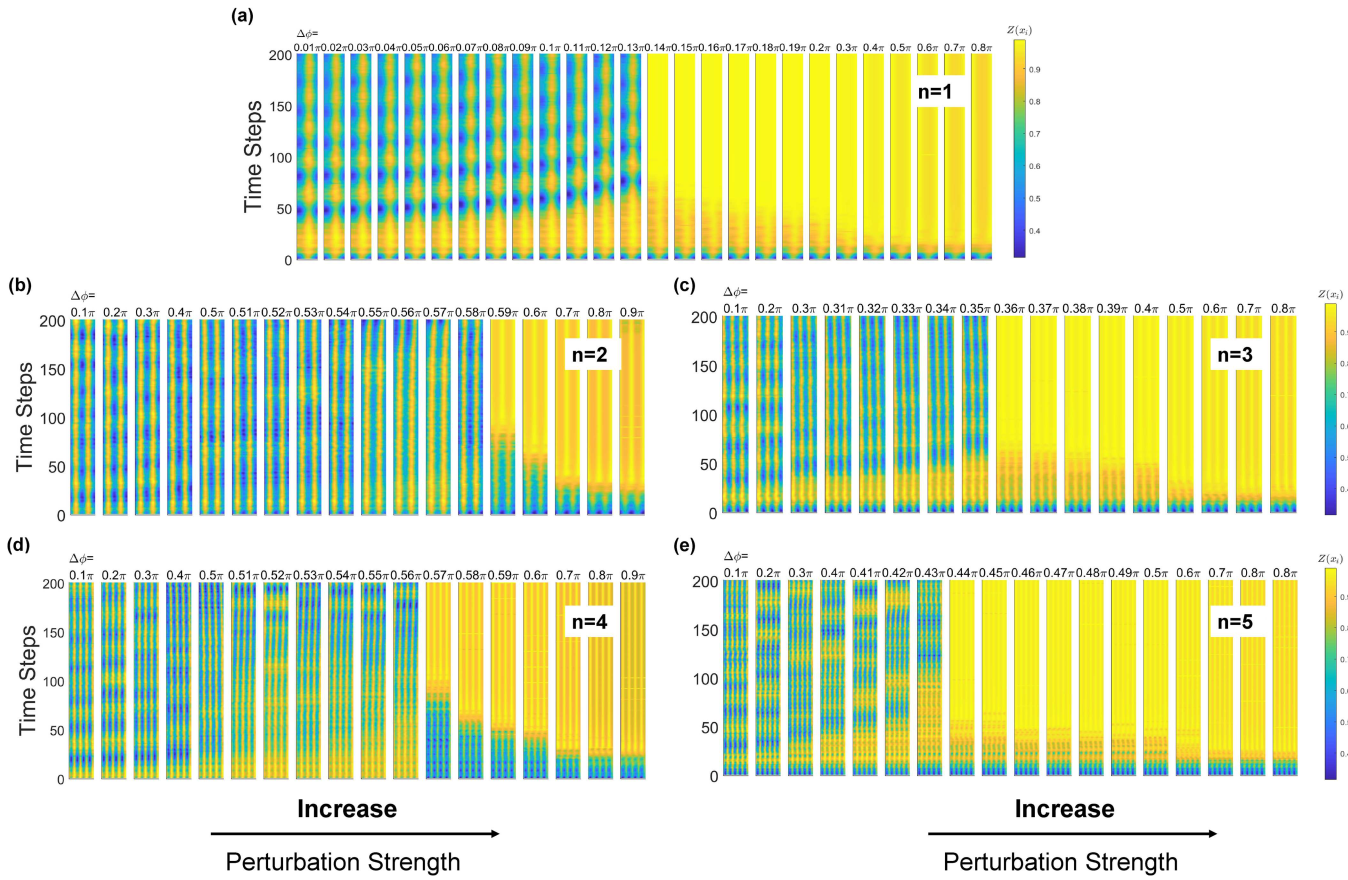

FIG. 1. Spatiotemporal patterns in response to each perturbation strength $\Delta\phi$ for system (1) are labeled above. The coherent and incoherent regions are represented by the yellow and blue colors, respectively. The cluster numbers of (a–e) are $n = 1$–5. The system is of size $N = 240$, and each perturbation is applied to four oscillators beside one of the coherent centers of that system. (a) For chimera with cluster number $n = 1$, the coherent center is $m_c = 127$, and the target oscillators are $m_1 = 126$, $m_2 = 127$, $m_3 = 128$, $m_4 = 129$. (b) For 2-cluster chimera, the coherent centers are $m_{c1} = 52$ and $m_{c2} = 172$. Then, $m_{c1} = 52$ was chosen randomly, and perturbations are applied upon oscillators $m_1 = 51$, $m_2 = 52$, $m_3 = 53$, and $m_4 = 54$. (c) For 3-cluster chimera, the selected coherent center is $m_{c1} = 24$, and the targets are $m_1 = 23$, $m_2 = 24$, $m_3 = 25$, and $m_4 = 26$. (d) For 4-cluster chimera, the selected coherent center is $m_{c1} = 24$, and the targets are $m_1 = 49$, $m_2 = 50$, $m_3 = 51$, and $m_4 = 52$. (e) For 5-cluster chimera, the selected coherent center is $m_{c2} = 40$, and the targets are $m_1 = 39$, $m_2 = 40$, $m_3 = 41$, and $m_4 = 42$, respectively.

we have also conducted a comparative analysis of critical values, procedures of phase transitions, and the transient time among different cluster structures. These difference well describe anti-interference capabilities and robustness of different chimera structures. We conjecture that the larger the perturbation critical value $\Delta\phi_c$ is, the stronger anti-interference ability of the structure would have.

The critical values of 1, 2, 3, 4, 5-cluster chimera averaged over ten different initial states are $\Delta\phi_{c1} = 0.133\pi$, $\Delta\phi_{c2} = 0.586\pi$, $\Delta\phi_{c3} = 0.355\pi$, $\Delta\phi_{c4} = 0.564\pi$, and $\Delta\phi_{c5} = 0.449\pi$. Apparently, the order of them is $\Delta\phi_{c1} < \Delta\phi_{c3} < \Delta\phi_{c5} < \Delta\phi_{c4} < \Delta\phi_{c2}$, and one can also imagine that $\Delta\phi_{c(2n)} = \Delta\phi_{c(2n-1)}$ as $n \to \infty$. Based on this measurement, we conjecture that the anti-interference capability of odd-numbered clusters is weaker than that of even-numbered clusters. Specifically, the stability of 2-cluster chimera is much stronger than others, while 1-cluster chimera is most unstable.

C. Criticality observed from transient time

The transient time (T) that denotes the duration for the system to achieve a stable state of either chimera or synchronization is plotted in Fig. 2 as a function of perturbation strength $\Delta\phi$. The variation trend of T on both sides of the critical value $\Delta\phi_c$ behaves generally the same for the chimera with different numbers of clusters. Figure 2 shows the results from the systems with ten different initial states, and the qualitative tendency for the transient time T is basically the same. To eliminating the influence of initials and make the changing characteristic clearer, we subtract the critical values $\Delta\phi_{cn}$ from the X axis of the transient time curve and perform a translation. In this way, curves were centralized, and X axis describes the distance between the perturbation strength and the critical value ($X = \Delta\phi - \Delta\phi_c$) as shown in Fig. 3, and $X = 0$ corresponds to the critical point.

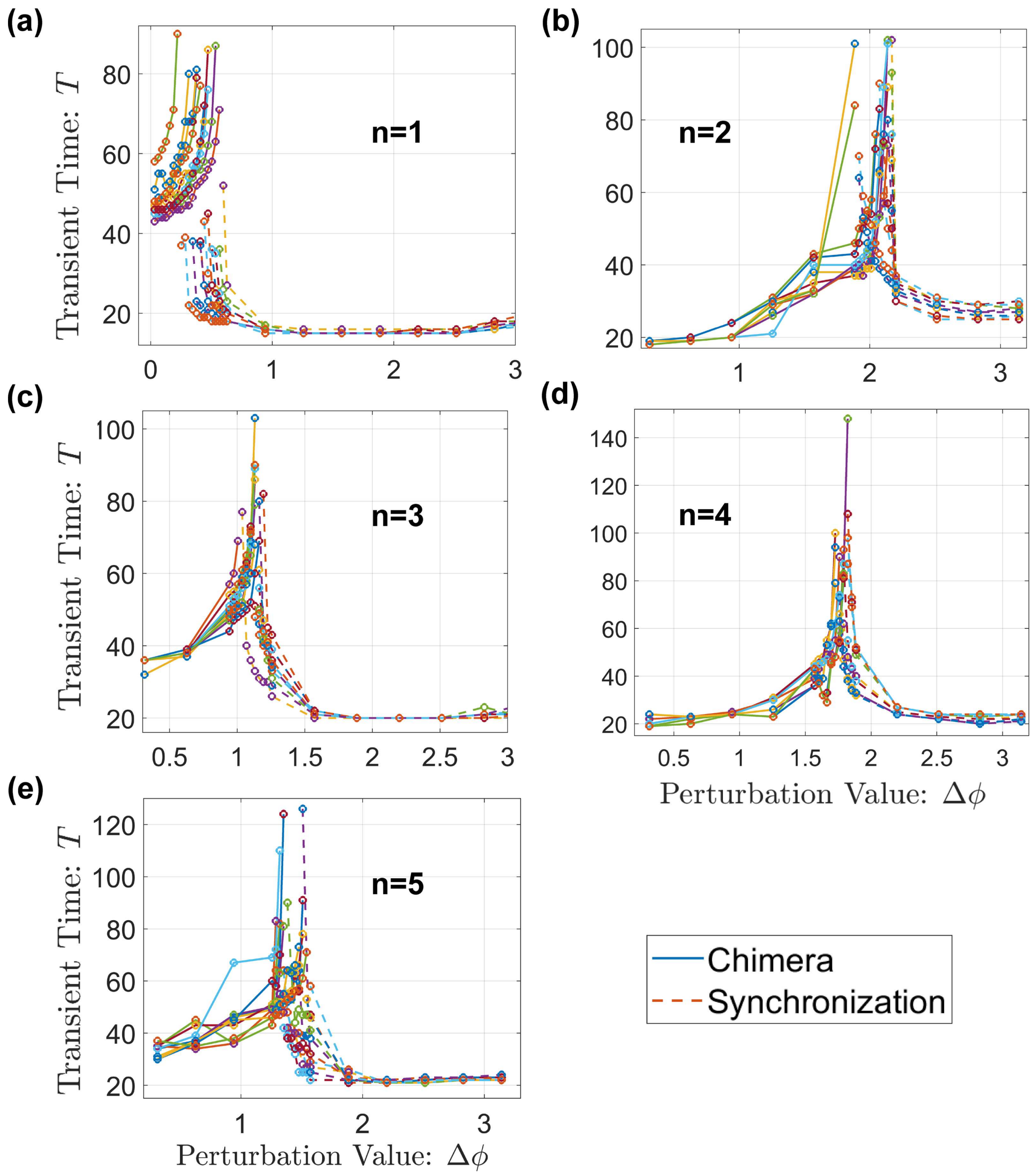

FIG. 2. The transient time under perturbations. The solid lines describe transient times toward chimera, while the dotted lines describe those toward synchronization. The parameter n represents the cluster number of chimera states: (a) transient time of the 1-cluster chimera in response to perturbations, (b) transient time of the 2-cluster chimera, (c) transient time of the 3-cluster chimera, (d) transient time of the 4-cluster chimera, and (e) transient time of the 5-cluster chimera. Each figure has ten pairs of lines, representing the averaged measurement from different initial groups.

Specifically speaking, when the perturbation strength approaches the critical value on the left, the transient time toward chimera increases rapidly according to a power law. However, when the perturbation strength is larger than the critical value and keeps increasing, the transient time of synchronization decays rapidly in the form of another power-law distribution. Moreover, the transient time approaches infinity around the critical point. In order to find the power-law distribution that the transient time toward two states obeys, we average the original data and present it in a log–log plot. We use least squares fitting to estimate the parameters in the power-law relationship on the logarithmic scale, i.e., $log(\bar{T}) = -\alpha log(X) + log(C)$ (see Fig. 4) or $\bar{T} \sim C(\Delta\phi - \Delta\phi_c)^{-\alpha}$, and the fitting error R^2 can be adopted to judge the goodness of the fitting (shown in Tables I and II). One can see that the magnitude of their exponents is in the same order of the critical value: $\alpha_1 < \alpha_3 < \alpha_5 < \alpha_4 < \alpha_2$. Moreover, the order of $\bar{T}$'s variation range

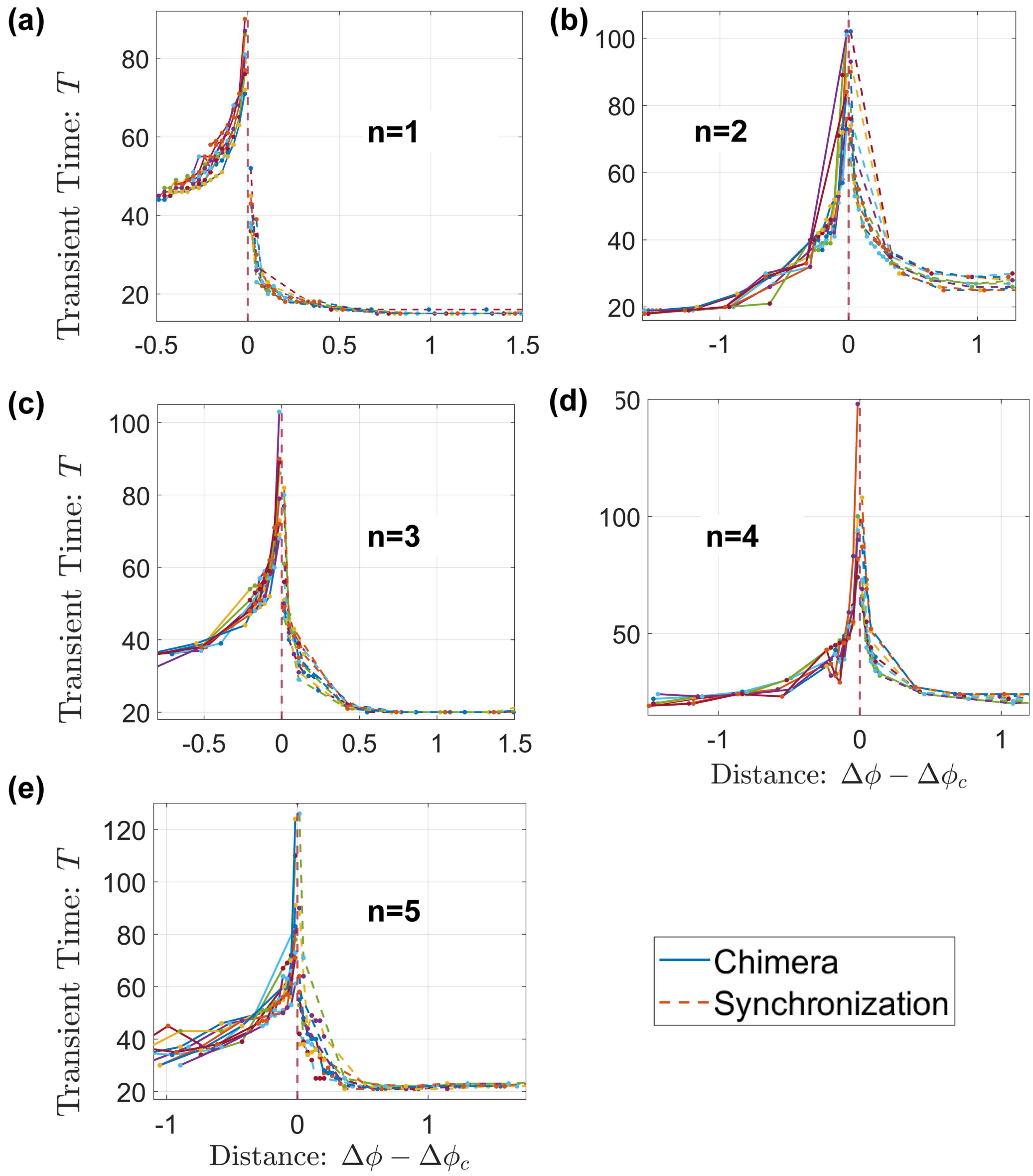

FIG. 3. Averaged transient time, corresponding to the distance between perturbation strength and the critical value ($X = \Delta\phi - \Delta\phi_c$), which is zero-centered. The solid lines describe the transient time toward chimera, while the dotted lines describe the transient time toward synchronization. The parameter *n* in figures represents the cluster number of the chimera system: (a) transient time of the 1-cluster chimera in response to perturbations, (b) transient time of the 2-cluster chimera, (c) transient time of the 3-cluster chimera, (d) Transient time of the 4-cluster chimera, and (e) transient time of the 5-cluster chimera. Each figure has ten pairs of lines, representing the averaged measurement from different initial groups.

is also the same: $\Delta\bar{T}_1 < \Delta\bar{T}_3 < \Delta\bar{T}_5 < \Delta\bar{T}_4 < \Delta\bar{T}_2$. It means that the larger the critical value, the larger the variation range of the transient time, and the higher the stability and robustness of the system.

Meanwhile, the transient time before entering the synchronization can also be well fitted by a power-law distribution, but more interestingly, for each cluster case, when the perturbation strength increases, the transient time decreases in a power law with similar power exponents, which are all approximately equal to 0.27. However, values of the fitted intercepts have the same order as the critical values, which is $C_1 < C_3 < C_5 < C_4 < C_2$. This phenomenon well indicates that if the system has stronger anti-disturbance ability, the transient time toward synchronization will have a larger range and the convergence value consequently. Based on this finding, we can

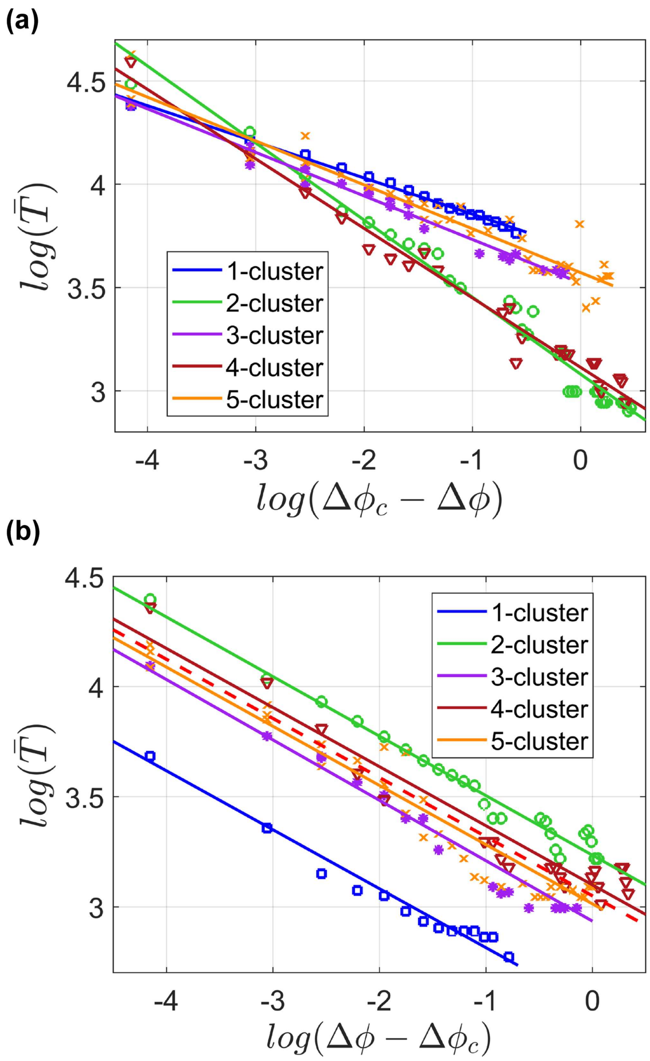

FIG. 4. Transient time in logarithmic coordinates. (a) The transient time toward chimera in logarithmic coordinates, where points are measured values and the solid lines are fitted models. (b)The transient time toward synchronization in logarithmic coordinates, where points are measured values and the solid lines are fitted models. The red dotted line is the predicted distribution in n-cluster chimera ($n \to \infty$).

TABLE I. Parameters and fitted distributions of the transient time toward chimera for the n-cluster cases.

n	Slope	Fitted distribution	R^2
1	−0.175	$y = =39.646x^{-0.175}$	0.994
3	−0.211	$y = =33.852x^{-0.211}$	0.988
5	−0.212	$y = =35.588x^{-0.212}$	0.925
4	−0.336	$y = =22.488x^{-0.336}$	0.979
2	−0.373	$y = =21.780x^{-0.373}$	0.977

TABLE II. Parameters and fitted distributions of transient time toward synchronization for the n-cluster cases.

n	Slope	Fitted distribution	R^2
1	−0.268	$y = 12.770x^{-0.268}$	0.963
3	−0.274	$y = 18.825x^{-0.274}$	0.963
5	−0.272	$y = 20.180x^{-0.272}$	0.928
4	−0.268	$y = 22.189x^{-0.268}$	0.928
2	−0.270	$y = 25.392x^{-0.270}$	0.974

predict the distribution of the transient time toward synchronization for an n-cluster chimera with $n \to \infty$, which is represented by the red dashed line in Fig. 4(b).

IV. THEORETICAL ANALYSIS OF THE CRITICAL VALUE

A. Comparison and assumption

After centered the perturbation strength and averaged the transient time of ten initial groups, we can compare the critical value of n-cluster chimera ($n = 1, 2, 3, 4, 5$) in the same coordinate system as shown in Fig. 5.

According to the above results and figures, we found an interesting phenomenon, that is, as the number of clusters increases, the difference between critical values becomes smaller and smaller, which reminds us of the Feigenbaum constant $[\delta = \lim_{n\to\infty}(a_{n-1} - a_{n-2})/(a_n - a_{n-1}) \cdots]$ in the period-doubling bifurcation, which expresses the limit of the ratio of distances between consecutive bifurcation diagram.[81] Therefore, we suppose that as the cluster number approaches infinity, the critical values of odd and even clusters will converge into the same value from

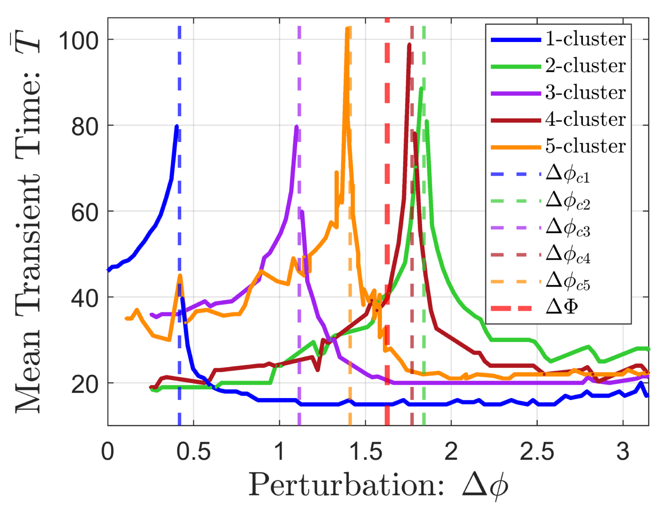

FIG. 5. Comparison of the critical values and the changing trend of the transient time toward chimera and synchronization. In this way, the order of critical values is represented clearly: $\Delta\phi_{c1} < \Delta\phi_{c3} < \Delta\phi_{c5} < \Delta\phi_{c4} < \Delta\phi_{c2}$. Moreover, the red dotted line is a prediction of n-cluster chimera's critical value with $n \to \infty$, denoted by $\Delta\Phi$, which is obtained based on the convergence phenomenon.

two sides in two proportional sequences. A crude estimation of the common ratio of critical values of odd clusters is q_1, which can be calculated by $q_1 = a_2/a_1 = (\Delta\phi_{c5} - \Delta\phi_{c3})/(\Delta\phi_{c3} - \Delta\phi_{c1})$. Then, based on the summation formula of the proportional series: $S_1 = a_1(1 - q_1^n)/(1 - q_1)$, as $n \to +\infty$, we can predict the critical value of the n-cluster chimera by $\Delta\Phi = \Delta\phi_{c1} + a_1/(1 - q_1)$. After that, the common ratio of even clusters q_2 can be obtained from $S_2 = \Delta\phi_{c2} - \Delta\Phi = b_1/(1 - q_2)$, that is, $q_2 = 1 - b_1/(\Delta\phi_{c2} - \Delta\Phi)$.

First, using critical values from our experiments, we have $a_1 = \Delta\phi_{c3} - \Delta\phi_{c1} = 0.222\pi, a_2 = \Delta\phi_{c5} - \Delta\phi_{c3} = 0.094\pi, b_1 = \Delta\phi_{c2} - \Delta\phi_{c4} = 0.022\pi$, and $q_1 = \frac{a_2}{a_1} = 0.4234$ consequently. Thus, the predicted critical value of the n-cluster chimera with $n \to \infty$ is

$$\Delta\Phi \equiv \overline{\lim_{i\to\infty}} \Delta\phi_{c(2i+1)} = \underline{\lim_{i\to\infty}} \Delta\phi_{c(2i)}$$

$$= \Delta\phi_{c1} + a_1 \frac{1}{1 - q_1} = 0.518\pi.$$

$S_2 = \Delta\phi_{c2} - \Delta\Phi = 0.068\pi$ and $q_2 = 1 - 0.022\pi/S_2 = 0.6763$ are obtained. Moreover, based on the relationship $S_1 + S_2 = a_1/(1 - q_1) + b_1/(1 - q_2) = (\Delta\phi_{c2} - \Delta\phi_{c1})$, we can derive a relation equation between q_1 and q_2, that is, $0.222/(1 - q_1) + 0.022/(1 - q_2) = 0.453$. As the assumption stated above, this convergence process is demonstrated in Fig. 6.

B. Deviation analysis

From the assumption above, we can predict the critical value of the n-cluster chimera, using $\Delta\phi_{c1}, \Delta\phi_{c2}, \Delta\phi_{c3}, \Delta\phi_{c4}, \Delta\phi_{c5}$ that we obtained in experiments. However, there exists a standard deviation for each calculated critical values $\sigma_{c1} = 0.0327, \sigma_{c2} = 0.0126, \sigma_{c3} = 0.0135, \sigma_{c4} = 0.0117, \sigma_{c5} = 0.0574$. Therefore, the predicted $\Delta\Phi$ has a standard deviation σ_c either, which can be calculated by using the error transfer formula of mathematical statistics. The procedures are as follows:

We already know that $\Delta\Phi = \Delta\phi_{c1} + a_1 \frac{1}{1-q_1}$. Thus, based on the error transfer formula, we have

$$\sigma_c^2 = \sigma_{c1}^2 + \sigma_{\frac{a_1}{1-q_1}}^2,$$

$$\sigma_{a_1}^2 = \sigma_{c1}^2 + \sigma_{c3}^2;\ \sigma_{a_2}^2 = \sigma_{c5}^2 + \sigma_{c3}^2,$$

$$\sigma_{a_1-a_2}^2 = \sigma_{a_1}^2 + \sigma_{a_2}^2,$$

$$\sigma_{1-q_1}^2 = \sigma_{\frac{a_1-a_2}{a_1}}^2 = \left(\frac{\sigma_{a_1-a_2}}{a_1 - a_2}\right)^2 + \left(\frac{\sigma_{a_1}}{a_1}\right)^2,$$

$$\sigma_{\frac{a_1}{1-q_1}}^2 = \left(\frac{\sigma_{a_1}}{a_1}\right)^2 + \left(\frac{\sigma_{1-q_1}}{1 - q_1}\right)^2,$$

$$\sigma_c^2 = \sigma_{c1}^2 + \left[\frac{1}{a_1^2} + \frac{1}{(1-q_1)^2}\left(\frac{1}{(a_1-a_2)^2} + \frac{1}{a_1^2}\right)\right](\sigma_{c1}^2 + \sigma_{c3}^2)$$
$$+ \frac{1}{(1-q_1)^2(a_1-a_2)^2}(\sigma_{c5}^2 + \sigma_{c3}^2) = 0.9718.$$

The standard deviation of n-cluster's critical value with $n \to \infty$, i.e., the standard deviation of $\Delta\Phi$ is $\sigma_c = 0.9858$.

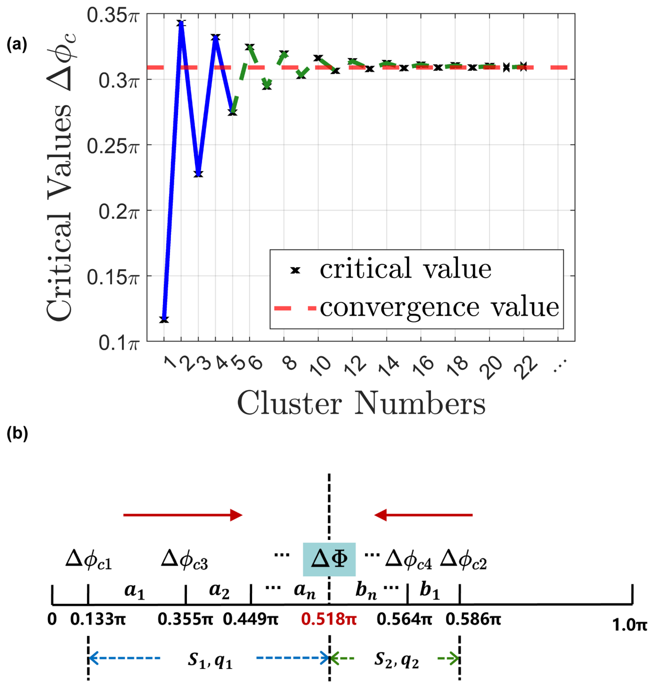

FIG. 6. The convergence process. (a) The X axis is the number of clusters, while the Y axis corresponds to the critical value. As the cluster number approaches infinity, the critical value of odd and even clusters will converge into a certain value from two sides in two proportional sequences. (b) is a schematic illustration of the convergence process. $\Delta\phi_{ci}$ is the critical value of the i-cluster chimera, a_k is the difference between the critical value of the $(2k + 1)$ and $(2k - 1)$-cluster, and b_j is the difference between the critical value of the $2j$ and $(2j + 2)$-cluster$(i, k, j = 1, 2, 3, \cdots)$. q_1 and q_2 are common ratios of proportional sequences of odd and even clusters, respectively. The convergence direction is represented by red arrows.

C. Extension

To confirm the universality of the critical behavior of the transient time and the transion of the final stable state from chimera to sycronization, we conducted more simulation for the system of larger sizes. It was observed that with an increasing $\Delta\phi$, the transition behavior from a 1-cluster chimera or a 2-cluster chimera to synchronization was also quantitatively identical in larger-sized systems. Figure 7 illustrates the results of a system with $N = 480$. Furthermore, on both sides of the critical point $\Delta\phi_c$, which corresponds to the transition from the initial state to either the chimera state or the synchronized state, the transient behavior exhibits scaling characteristics. When the network size becomes larger, we find that an equivalent perturbation cannot be achieved by proportionally increasing the number of perturbed oscillators. The study of the number of perturbed oscillators is a topic that deserves further investigation in the future. In this paper, we only discuss the impact of increasing perturbation strength on transient behavior.

We have also attempted a scenario closer to the real Kuramoto model, in which the self-frequencies ω_i of each oscillator were not

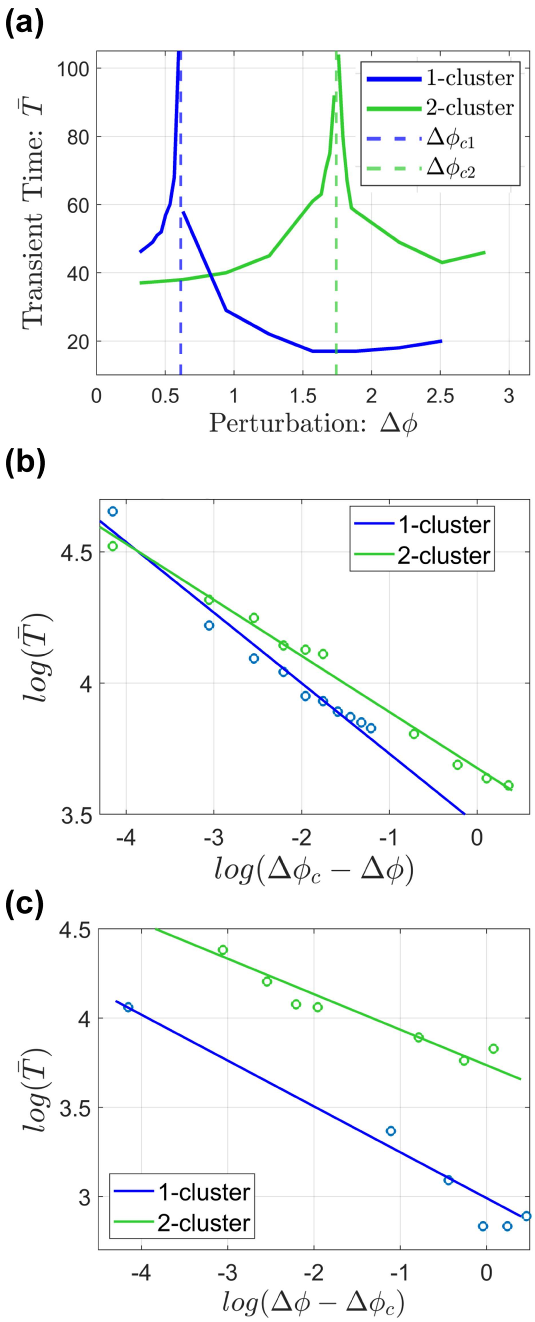

FIG. 7. Transient time for the system with $N = 480$. (a) Transition from chimera to synchronization as $\Delta\phi$ increases through the critical value marked by the dashed line, for the system with the number of clusters to be 1 (blue curves) and 2 (green curves), respectively. (b) The transient time toward chimera in logarithmic coordinates, where points are measured values and the solid lines are the linear fittings. The fitted slopes are -0.2685 (blue line) and -0.2134 (green line). (c) The transient time toward synchronization in logarithmic coordinates, where points are measured values and the solid lines are the linear fittings. The fitted slopes are -0.2570 (blue line) and -0.1990 (green line).

constant but randomly selected from a Gaussian distribution with different standard deviations. The formation conditions for the chimera state are quite stringent, as the chimera state can only be formed when the ω_i values are completely identical (homogeneous). As the standard deviation σ of the Gaussian distribution $N(0, \sigma^2)$ used for sampling the ω_i values increases, it indicates a higher degree of heterogeneity, and the disorderliness of the system also gradually increases. From the spatiotemporal pattern in Fig. 8, we may find that when the standard deviation of the Gaussian distribution (representing the heterogeneity of ω_i values) is non-zero, the system cannot form a stable chimera state. Moreover, as σ becomes larger, the system enters a disordered state. Therefore, due to the strict conditions for the existence of chimera, the transient time behavior of chimera and the transition from chimera to synchronization observed in simulations of identical oscillator systems would be difficult to observe in real Kuramoto systems, where the oscillators have non-identical ω_i values.

V. CONCLUSION AND DISCUSSION

In summary, we have numerically solved the coupled phase oscillator system of multi-chimera states $(1, 2, 3, 4, 5$-cluster chimera) upon phase perturbations, in order to investigate the critical behavior of the coupled oscillator system in the transient time toward chimera and synchronization.

First, we have introduced the definition of the transient time, experimental procedures, and measurement methods that we use. Next, based on our results, we have discussed how does the system respond to perturbations before entering the stable state and found that there is a critical value between chimera and synchronization that the system will get into. Once the perturbation strength is greater than the critical value, chimera will be taken over by synchronization. After fitting the changing trend of the transient time based on a log–log verification and the linear regression model, we have found that with the increase in the disturbance strength, the transient time obeys an increasing power-law distribution on the left-hand side of the critical value, and a decreasing power-law distribution on the right-hand side. In addition, we have shown that the parameters in the fitted model are associated with the critical value of this chimera.

Particularly, based on the comparison plots and the interesting phenomenon that the critical value of odd and even clusters will converge into a certain value from two sides in two proportional sequences, we have calculated the common ratio, made a prediction for the critical value of n-cluster chimera, and performed a deviation analysis finally. The mechanism for the transitions can be summarized as follows: chimera, asynchronization, and synchronization states have their own attraction basins, respectively, in the state space. For the classical synchronization transition through increasing coupling strength among oscillators,[82] the increase in coupling strength actually leads to the expansion of the attraction basin of the synchronization state, which, in turn, produces transition from asynchronization to synchronization. In our study, the transition from chimera to synchronization is induced by applying phase driving upon a small set of oscillators and, in fact, the phase driving does not change the attraction basins of chimera and synchronization,

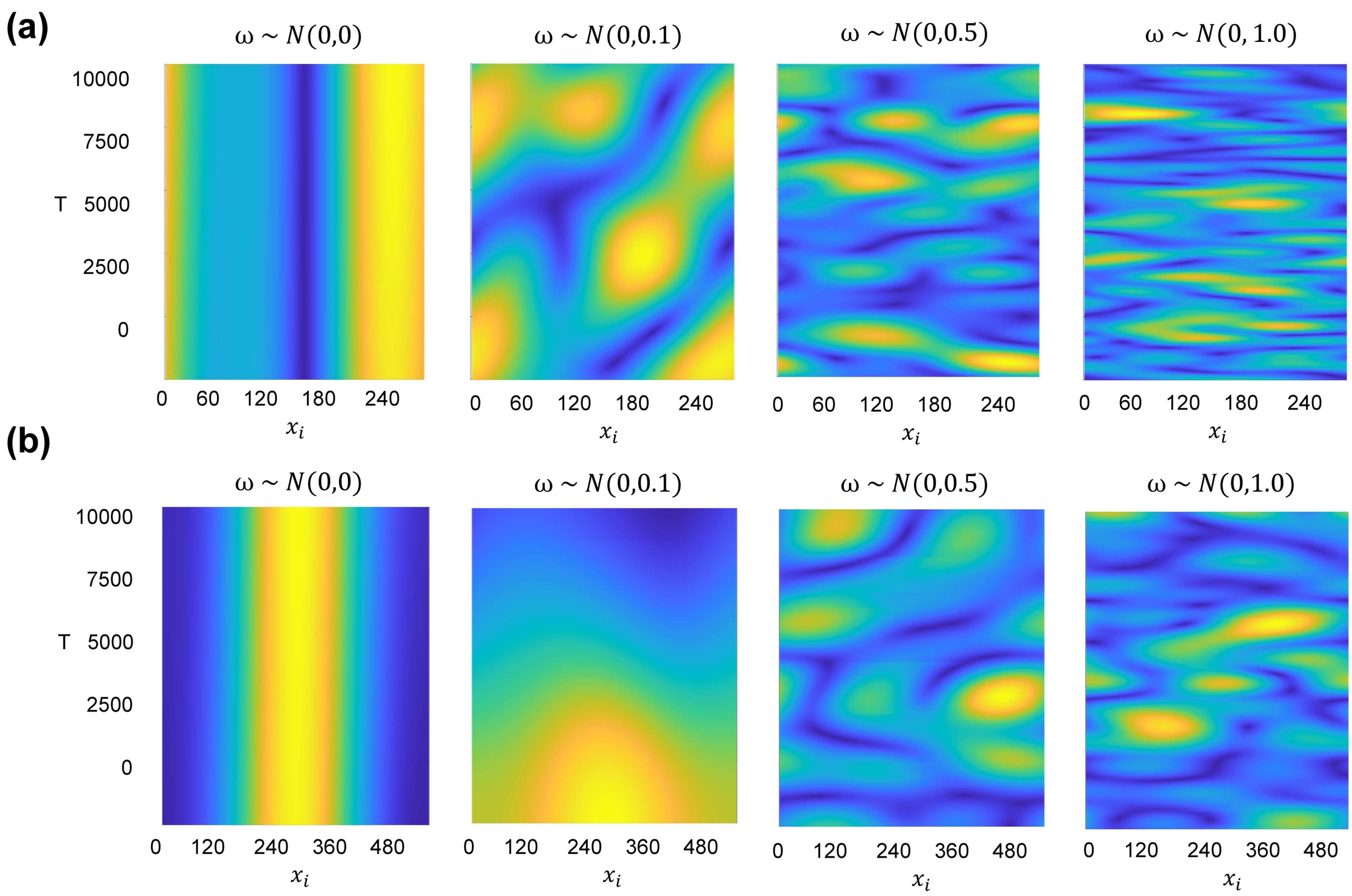

FIG. 8. Spatiotemporal patterns of systems with non-identical ω_i and different sizes. (a) $N = 240$, (b) $N = 480$. The self-frequencies ω_i of the oscillators are randomly selected from Gaussian distributions $N(0, \sigma^2)$ with different standard deviation σ. The x axis represents the oscillator index, and the y axis represents the evolution time steps.

but directly pulls the state of the system from the attraction basin of chimera to that of synchronization. Briefly speaking, the mechanism of transitions can be classified into two types, one is due to the change of the attraction basins, and the other is due to the change of state crossing the boundary of two different basins. The transitions in our work belong to the latter case.

ACKNOWLEDGMENT

We acknowledge helpful discussions with Prof. Ying-Cheng Lai and Dr. Si-Ping Zhang. This work was supported by the National Key R&D Program of China under Grant No. 2021ZD0201300, the Project Supported by Natural Science Basic Research Plan in Shaanxi Province of China (Program Nos. 2023-JC-YB-071, 2022JQ-010), Scientific Research Program Funded by Shaanxi Provincial Education Department (Program No. 22JP053), Shaanxi Fundamental Science Research Project for Mathematics and Physics (Grant No. 22JSQ037), NSFC of China (Grant No. 41975040), and the Taishan Industrial Experts Program.

AUTHOR DECLARATIONS

Conflict of Interest

The authors have no conflicts to disclose.

Author Contributions

Nan Yao: Conceptualization (equal); Data curation (equal); Formal analysis (equal); Funding acquisition (equal); Investigation (equal); Methodology (equal); Resources (equal); Validation (equal); Writing – review & editing (equal). **Qian-Yun Zhang:** Data curation (equal); Formal analysis (equal); Investigation (equal); Methodology (equal); Resources (equal); Software (equal); Visualization (equal); Writing – original draft (equal); Writing – review & editing (equal). **De-Yi Ren:** Formal analysis (equal); Methodology (equal). **You-Jun Li:** Funding acquisition (equal); Writing – review & editing (equal). **Chun-Wang Su:** Writing – review & editing (equal). **Zhong-Ke Gao:** Writing – review & editing (equal). **Jürgen Kurths:** Supervision (equal); Validation (equal).

DATA AVAILABILITY

The data that support the findings of this study are available from the corresponding author upon reasonable request.

REFERENCES

[1] Y. Kuramoto and D. Battogtokh, "Coexistence of coherence and incoherence in nonlocally coupled phase oscillators," Nonlinear Phenom. Complex Syst. **5**, 380–385 (2002).
[2] D. M. Abrams and S. H. Strogatz, "Chimera states for coupled oscillators," Phys. Rev. Lett. **93**, 174102 (2004).
[3] S.-I. Shima and Y. Kuramoto, "Rotating spiral waves with phase-randomized core in nonlocally coupled oscillators," Phys. Rev. E **69**, 036213 (2004).
[4] N. C. Rattenborg, C. J. Amlaner, and S. L. Lima, "Behavioral, neurophysiological and evolutionary perspectives on unihemispheric sleep," Neurosci. Biobehav. Rev. **24**, 817–842 (2000).
[5] R. Ma, J. Wang, and Z. Liu, "Robust features of chimera states and the implementation of alternating chimera states," Europhys. Lett. **91**, 40006 (2010).
[6] H. Sakaguchi, "Instability of synchronized motion in nonlocally coupled neural oscillators," Phys. Rev. E **73**, 031907 (2006).
[7] S. Olmi, A. Politi, and A. Torcini, "Collective chaos in pulse-coupled neural networks," Europhys. Lett. **92**, 60007 (2010).
[8] A. E. Motter, S. A. Myers, M. Anghel, and T. Nishikawa, "Spontaneous synchrony in power-grid networks," Nat. Phys. **9**, 191–197 (2013).
[9] J. Gonzalez-Avella, M. Cosenza, and M. S. Miguel, "Localized coherence in two interacting populations of social agents," Physica A **399**, 24–30 (2014).
[10] J. M. Davidenko, A. V. Pertsov, R. Salomonsz, W. Baxter, and J. Jalife, "Stationary and drifting spiral waves of excitation in isolated cardiac muscle," Nature **355**, 349–351 (1992).
[11] A. Rothkegel and K. Lehnertz, "Irregularmacroscopic dynamics due to chimera states in small-world networks of pulse-coupled oscillators," New J. Phys. **16**, 055006 (2014).
[12] D. M. Abrams and S. H. Strogatz, "Chimera states in a ring of nonlocally coupled oscillators," Int. J. Bifurcation Chaos **16**, 21–37 (2006).
[13] D. M. Abrams, R. Mirollo, S. H. Strogatz, and D. A. Wiley, "Solvable model for chimera states of coupled oscillators," Phys. Rev. Lett. **101**, 084103 (2008).
[14] E. A. Martens, "Chimeras in a network of three oscillator populations with varying network topology," Chaos **20**, 043122 (2010).
[15] E. A. Martens, C. R. Laing, and S. H. Strogatz, "Solvable model of spiral wave chimeras," Phys. Rev. Lett. **104**, 044101 (2010).
[16] Y. Maistrenko, O. Sudakov, O. Osiv, and V. Maistrenko, "Chimera states in three dimensions," New J. Phys. **17**, 073037 (2015).
[17] M. J. Panaggio and D. M. Abrams, "Chimera states on a flat torus," Phys. Rev. Lett. **110**, 094102 (2013).
[18] O. E. Omel'chenko, M. Wolfrum, S. Yanchuk, Y. L. Maistrenko, and O. Sudakov, "Stationary patterns of coherence and incoherence in two-dimensional arrays of non-locally-coupled phase oscillators," Phys. Rev. E **85**, 036210 (2012).
[19] M. J. Panaggio and D. M. Abrams, "Chimera states on the surface of a sphere," Phys. Rev. E **91**, 022909 (2015).
[20] O. E. Omel'chenko, M. Wolfrum, and Y. L. Maistrenko, "Chimera states as chaotic spatiotemporal patterns," Phys. Rev. E **81**, 065201 (2010).
[21] M. Wolfrum and O. E. Omel'chenko, "Chimera states are chaotic transients," Phys. Rev. E **84**, 015201 (2011).
[22] M. Wolfrum, O. E. Omel'chenko, S. Yanchuk, and Y. L. Maistrenko, "Spectral properties of chimera states," Chaos **21**, 013112 (2011).
[23] J. H. Sheeba, V. K. Chandrasekar, and M. Lakshmanan, "Globally clustered chimera states in delay-coupled populations," Phys. Rev. E **79**, 055203 (2009).
[24] G. C. Sethia, A. Sen, and F. M. Atay, "Clustered chimera states in delay-coupled oscillator systems," Phys. Rev. Lett. **100**, 144102 (2008).
[25] O. E. Omel'chenko, Y. L. Maistrenko, and P. A. Tass, "Chimera states: The natural link between coherence and incoherence," Phys. Rev. Lett. **100**, 044105 (2008).
[26] Y. Zhu, Y. Li, M. Zhang, and J. Yang, "The oscillating two-cluster chimera state in non-locally coupled phase oscillators," Europhys. Lett. **97**, 10009 (2012).
[27] Y. Lei, X.-J. Xu, X. Wang, Y. Zou, and J. Kurths, "A new criterion for optimizing synchrony of coupled oscillators," Chaos, Solitons Fractals **168**, 113192 (2023).
[28] I. Omelchenko, E. Omel'chenko, P. Hövel, and E. Schöll, "When nonlocal coupling between oscillators becomes stronger: Patched synchrony or multichimera states," Phys. Rev. Lett. **110**, 224101 (2013).
[29] S. R. Ujjwal and R. Ramaswamy, "Chimeras with multiple coherent regions," Phys. Rev. E **88**, 032902 (2013).
[30] Y. Zhu, Z. Zheng, and J. Yang, "Reversed two-cluster chimera state in nonlocally coupled oscillators with heterogeneous phase lags," Europhys. Lett. **103**, 10007 (2013).
[31] Y. Zhang and A. E. Motter, "Mechanism for strong chimeras," Phys. Rev. Lett. **126**, 094101 (2021).
[32] S. Kundu and D. Ghosh, "Higher-order interactions promote chimera states," Phys. Rev. E **105**, L042202 (2022).
[33] M. I. Bolotov, L. A. Smirnov, G. V. Osipov, and A. Pikovsky, "Locking and regularization of chimeras by periodic forcing," Phys. Rev. E **102**, 042218 (2020).
[34] C. R. Laing, K. Rajendran, and I. G. Kevrekidis, "Chimeras in random noncomplete networks of phase oscillators," Chaos **22**, 013132 (2012).
[35] N. Yao, Z.-G. Huang, Y.-C. Lai, and Z.-G. Zheng, "Robustness of chimera states in complex dynamical systems," Sci. Rep. **3**, 3522 (2013).
[36] Y. Zhu, Z. Zheng, and J. Yang, "Chimera states on complex networks," Phys. Rev. E **89**, 022914 (2014).
[37] N. Yao, Z.-G. Huang, C. Grebogi, and Y.-C. Lai, "Emergence of multicluster chimera states," Sci. Rep. **5**, 12988 (2015).
[38] A. D. Kachhvah and S. Jalan, "Explosive synchronization and chimera in interpinned multilayer networks," Phys. Rev. E **104**, L042301 (2021).
[39] M. Asllani, B. A. Siebert, A. Arenas, and J. P. Gleeson, "Symmetry-breaking mechanism for the formation of cluster chimera patterns," Chaos **32**, 013107 (2022).
[40] R. C. Budzinski, T. T. Nguyen, J. Doàn, J. Mináč, T. J. Sejnowski, and L. E. Muller, "Geometry unites synchrony, chimeras, and waves in nonlinear oscillator networks," Chaos **32**, 031104 (2022).
[41] T. Lilienkamp and U. Parlitz, "Susceptibility of transient chimera states," Phys. Rev. E **102**, 032219 (2020).
[42] Y. L. M. O. E. Omel'chenko and P. A. Tass, "Chimera states induced by spatially modulated delayed feedback," Phys. Rev. E **82**, 066201 (2010).
[43] A. P. G. Bordyugov and M. Rosenblum, "Self-emerging and turbulent chimeras in oscillator chains," Phys. Rev. E **82**, 35205 (2010).
[44] Y. Kawamura, "Chimera ising walls in forced nonlocally coupled oscillators," Phys. Rev. E **75**, 056204 (2007).
[45] A. S. G. C. Sethia and G. L. Johnston, "Amplitude-mediated chimera states," Phys. Rev. E **88**, 042917 (2013).
[46] G. C. Sethia and A. Sen, "Chimera states: The existence criteria revisited," Phys. Rev. Lett. **112**, 144101 (2014).
[47] M. K. A. Zakharova and E. Schöll, "Chimera death: Symmetry breaking in dynamical networks," Phys. Rev. Lett. **112**, 154101 (2014).
[48] K. Sathiyadevi, V. K. Chandrasekar, and M. Lakshmanan, "Emerging chimera states under nonidentical counter-rotating oscillators," Phys. Rev. E **105**, 034211 (2022).
[49] H. Bi and T. Fukai, "Amplitude-mediated chimera states in nonlocally coupled Stuart–Landau oscillators," Chaos **32**, 083125 (2022).
[50] P. H. I. Omelchenko, Y. Maistrenko, and E. Schöll, "Loss of coherence in dynamical networks: Spatial chaos and chimera states," Phys. Rev. Lett. **106**, 234102 (2011).
[51] D. Viennot and L. Aubourg, "Quantum chimera states," Phys. Lett. A **380**, 678–683 (2016).
[52] H.-Y. Xu, G.-L. Wang, L. Huang, and Y.-C. Lai, "Chaos in dirac electron optics: Emergence of a relativistic quantum chimera," Phys. Rev. Lett. **120**, 124101 (2018).
[53] G. S. E. S. S. Bogomolov, A. Slepnev, and V. S. Anishchenko, "Mechanisms of appearance of amplitude and phase chimera states in ensembles of nonlocally coupled chaotic systems," Commun. Nonlinear Sci. Numer. Simul. **43**, 25–36 (2017).
[54] P. H. Y. M. I. Omelchenko, B. Riemenschneider, and E. Schöll, "Transition from spatial coherence to incoherence in coupled chaotic systems," Phys. Rev. E **85**, 026212 (2012).

[55] N. Semenova, A. Zakharova, E. Schöll, and V. Anishchenko, "Does hyperbolicity impede emergence of chimera states in networks of nonlocally coupled chaotic oscillators?," Europhys. Lett. **112**, 40002 (2015).
[56] P. H. E. A. I. Omelchenko and O. E. Omel'chenko, "When nonlocal coupling between oscillators becomes stronger: Patched synchrony or multichimera states," Phys. Rev. Lett. **110**, 224101 (2013).
[57] I. O. E. A. A. Vüllings and J. Hizanidis, "Clustered chimera states in systems of type-I excitability," New J. Phys. **16**, 123039 (2014).
[58] H. Sakaguchi, "Instability of synchronized motion in nonlocally coupled neural oscillators," Phys. Rev. E **73**, 031907 (2006).
[59] Z. Lei, S. Pu, H. Zhang, C. Yao, Y. Qian, and Z. Zheng, "Bistability-induced chimeras in one-dimensional paced excitable rings with nonlocal couplings," Europhys. Lett. **139**, 62001 (2022).
[60] A. M. Hagerstrom, T. E. Murphy, R. Roy, P. Hövel, I. Omelchenko, and E. Schöll, "Experimental observation of chimeras in coupled-map lattices," Nat. Phys. **8**, 658 (2012).
[61] J. D. Hart, K. Bansal, T. E. Murphy, and R. Roy, "Experimental observation of chimera and cluster states in a minimal globally coupled network," Chaos **26**, 095801 (2016).
[62] M. R. Tinsley, S. Nkomo, and K. Showalter, "Chimera and phase-cluster states in populations of coupled chemical oscillators," Nat. Phys. **8**, 662 (2012).
[63] S. Nkomo, M. R. Tinsley, and K. Showalter, "Chimera states in populations of nonlocally coupled chemical oscillators," Phys. Rev. Lett. **110**, 244102 (2013).
[64] S. Nkomo, M. R. Tinsley, and K. Showalter, "Chimera and chimera-like states in populations of nonlocally coupled homogeneous and heterogeneous chemical oscillators," Chaos **26**, 094826 (2016).
[65] E. A. Martens, S. Thutupalli, A. Fourrière, and O. Hallatschek, "Chimera states in mechanical oscillator networks," Proc. Natl. Acad. Sci. U.S.A. **110**, 10563–10567 (2013).
[66] L. Larger, B. Penkovsky, and Y. Maistrenko, "Virtual chimera states for delayed-feedback systems," Phys. Rev. Lett. **111**, 054103 (2013).
[67] L. Schmidt, K. Schönleber, K. Krischer, and V. García-Morales, "Coexistence of synchrony and incoherence in oscillatory media under nonlinear global coupling," Chaos **24**, 013102 (2014).
[68] M. Wickramasinghe and I. Z. Kiss, "Spatially organized dynamical states in chemical oscillator networks: Synchronization, dynamical differentiation, and chimera patterns," PLoS One **8**, 0080586 (2013).
[69] J. B. Xie, E. Knobloch, and H. C. Kao, "Multicluster and traveling chimera states in nonlocal phase-coupled oscillators," Phys. Rev. E **90**, 022919 (2014).
[70] D. Dudkowski, K. Czolczynski, and T. Kapitaniak, "Traveling chimera states for coupled pendula," Nonlinear Dyn. **95**, 1859–1866 (2019).
[71] Y. Suda and K. Okuda, "Breathing multichimera states in nonlocally coupled phase oscillators," Phys. Rev. E **97**, 042212 (2018).
[72] M. I. Bolotov, L. A. Smirnov, G. V. Osipov, and A. S. Pikovsky, "Breathing chimera in a system of phase oscillators," JETP Lett. **106**, 393–399 (2017).
[73] S. J. Guo, Q. Dai, H. Y. Cheng, H. H. Li, F. Xie, and J. Z. Yang, "Spiral wave chimera in two-dimensional nonlocally coupled Fitzhugh-Nagumo systems," Chaos, Solitons Fractals **114**, 394–399 (2018).
[74] M. Bataille-Gonzalez, M. G. Clerc, and O. E. Omel'chenko, "Moving spiral wave chimeras," Phys. Rev. E **104**, L022203 (2021).
[75] B. K. Bera, D. Ghosh, and T. Banerjee, "Imperfect traveling chimera states induced by local synaptic gradient coupling," Phys. Rev. E **94**, 012215 (2016).
[76] L. Larger, B. Penkovsky, and Y. Maistrenko, "Virtual chimera states for delayed-feedback systems," Phys. Rev. Lett. **111**, 054103 (2013).
[77] I. Omelchenko, A. Provata, J. Hizanidis, E. Schöll, and P. Hövel, "Robustness of chimera states for coupled Fitzhugh-Nagumo oscillators," Phys. Rev. E **91**, 022917 (2015).
[78] A.-K. Malchow, I. Omelchenko, E. Schöll, and P. Hövel, "Robustness of chimera states in nonlocally coupled networks of nonidentical logistic maps," Phys. Rev. E **98**, 012217 (2018).
[79] Q. Li, K. C. Larosz, D. Han, P. Ji, and J. Kurths, "Basins of attraction of chimera states on networks," Front. Physiol. **13**, 959431 (2022).
[80] N. Yao, Z.-G. Huang, H.-P. Ren, C. Grebogi, and Y.-C. Lai, "Self-adaptation of chimera states," Phys. Rev. E **99**, 010201 (2019).
[81] M. J. Feigenbaum, "Quantitative universality for a class of nonlinear transformations," J. Stat. Phys. **19**, 25–52 (1978).
[82] C. Xu, X. Wang, and P. S. Skardal, "Generic criterion for explosive synchronization in heterogeneous phase oscillator populations," Phys. Rev. Res. **4**, L032033 (2022).